SUPPLEMENTARY APPENDIX

Fenofibrate reduces osteonecrosis without affecting antileukemic efficacy in dexamethasone-treated mice

Emily R. Finch,[1] Monique A. Payton,[1] David A. Jenkins,[1] Xiangjun Cai,[1] Lie Li,[1] Seth E. Karol,[2] Mary V. Relling[1] and Laura J. Janke[3]

[1]Department of Pharmaceutical Sciences, St. Jude Children's Research Hospital; [2]Department of Oncology, St. Jude Children's Research Hospital and [3]Department of Pathology, Division of Comparative Pathology, St. Jude Children's Research Hospital, Memphis, TN, USA

 doi:10.3324/haematol.2020.252767

Received: March 18, 2020.

Accepted: July 6, 2020.

Pre-published: July 16, 2020.

Correspondence: *LAURA JANKE* - laura.janke@stjude.org

Supplement to Fenofibrate reduces osteonecrosis without affecting antileukemic efficacy in dexamethasone treated mice

Emily R. Finch[1], Monique A. Payton[1], David A. Jenkins[1], Xiangjun Cai[1], Lie Li[1], Seth E. Karol[2], Mary V. Relling[1], Laura J. Janke[3*]

1. Department of Pharmaceutical Sciences, St. Jude Children's Research Hospital, Memphis, TN
2. Department of Oncology, St. Jude Children's Research Hospital, Memphis, TN
3. Department of Pathology, Division of Comparative Pathology, St. Jude Children's Research Hospital, Memphis, TN

*Corresponding author:

Email: laura.janke@stjude.org (L.J.J.)

Supplemental Methods:

Mice:

Mice (up to 5/cage) were maintained in sterile microisolator cages (Micro Vent System 75 JAG, Allentown, NJ) and housed on ventilated racks in a temperature- and humidity-controlled room, a 12-hour light/dark cycle and with free access to food and water. Food was withheld prior to measurement of fasting serum triglycerides: serum triglycerides were measured after a 12-16 hour fast (food was withheld; mice had free access to water).

Evaluation of osteonecrosis and arteriopathy:

Evaluation of osteonecrosis and arteriopathy have been extensively described previously (1-5). Briefly, both femurs were collected, fixed in 10% formalin, decalcified in 10% formic acid, paraffin-embedded, sagittally sectioned beginning at the medial knee, and stained with hematoxylin and eosin. Osteonecrosis was evaluated by a board-certified veterinary pathologist (L.J.J.) for presence of empty lacunae, ghost or pyknotic nuclei in osteocytes in the bone trabeculae, and necrosis of the adjacent marrow and stromal elements (1-4); and scored from 0 (negative for osteonecrosis) to 200 (equivalent to 100% necrosis in both hind limbs) as described (5). Arteriopathy lesions were evaluated in arteriolar branches of the medial genicular artery on the surface of the distal femoral condyles (3) and scored from 0 (negative for arteriopathy) to 8 (thrombotic arteriopathy in both limbs) (5).

White adipose tissue:

White adipose tissue (WAT) was evaluated at sacrifice: perigonadal (representative of visceral fat) and inguinal (representative of posterior subcutaneous fat) fat pads were dissected and weighed at time of necropsy (6, 7).

Quantification of dexamethasone:

Plasma dexamethasone were measured at the end of treatment using HPLC-MS with a linear reportable range of (5.1–1275 nM), as previously described (8).

Quantification of fenofibrate/fenofibric acid:

Quantitation of fenofibrate and analytes was carried out with a Waters ACQUITY separation system (Milford, MA) and Xevo TQ triple-quadrupole system (Beverly, MA). Separation was achieved on a Waters ACQUITY BEHC_{18} column (1.7 µm, 50 x 2.1 mm) using a column heater operating at 40°C with a Waters ACQUITY in-line filter. Autosampler temperature was maintained at 15° ± 5°C. The gradient mobile phase was composed of 0.1% formic acid of acetonitrile (B) and 0.1 % formic acid water (A). The flow rate was 0.6 ml/min, and the separation was completed within 5 min. The instrument was equipped with an electrospray interface, and was controlled by Masslynx 4.1 software (Waters, MA). The analysis was performed in MRM mode: *m/z* 361 > 232 for fenofibrate; *m/z* 318 > 232 for fenofibric acid; m/z 367> 234 for fenofibrate_d6; m/z 324>138 for fenofibric acid_d6. The MS/MS conditions were as follows: capillary voltage: 2.5kV; source temperature: 150°C; desolvation temperature: 500°C; cone gas flow: 0 l/h; desolvation gas flow: 1000 l/h. Note that no fenofibrate was detectable in our experimental samples.

Frozen samples were thawed at room temperature. A 10 µL aliquot of standard, QC or mouse sample was spiked into a polypropylene microcentrifuge tube and 30 µL of internal standard solution (5 ng/ml of fenofibrate and 25 ng/mL fenofibric acid in MeOH) was added. The tube was vortex-mixed for 20 sec, followed by centrifugation at 15,000 rpm for 8 min at 4°C. The supernatant was transferred to sample vial and 1µL was injected for analysis.

BCR-ABL model:

The BCR-ABL ($p185^{+}$, $Arf^{-/-}$) luciferase-positive cell line ($BCR\text{-}ABL^{+}$) was generated (8-11) . Female 8-week-old matched syngeneic mice (C57Bl/6J, *Arf*-wildtype; Jackson Laboratory, ME) received intravenous injections of 2000 $BCR\text{-}ABL^{+}$ cells. Bioluminescent imaging was performed weekly (8), to monitor leukemic burden. At day 3, mice were stratified by luminescent signal and body weight to treatment (n=10/treatment group). Fasting serum triglycerides were measured at day 24. Treatment ended at day 28: mice were maintained on base-diet/base-water until humane endpoint or the end of study at day 63. Mice were observed daily and sacrificed when luminescence was nearing saturation (pre-determined ventral-luminescence threshold of $1x10^{10}$) or they displayed clinical signs (hind limb paralysis, ruffled fur, respiratory distress, poor mobility) or at the end of study at day 63. Peripheral white blood cell count (WBC) and spleen weight were measured at sacrifice. In both the control and dexamethasone-only treatment groups, one mouse was censored from analysis due to early death not related to leukemia.

Supplemental Figures:

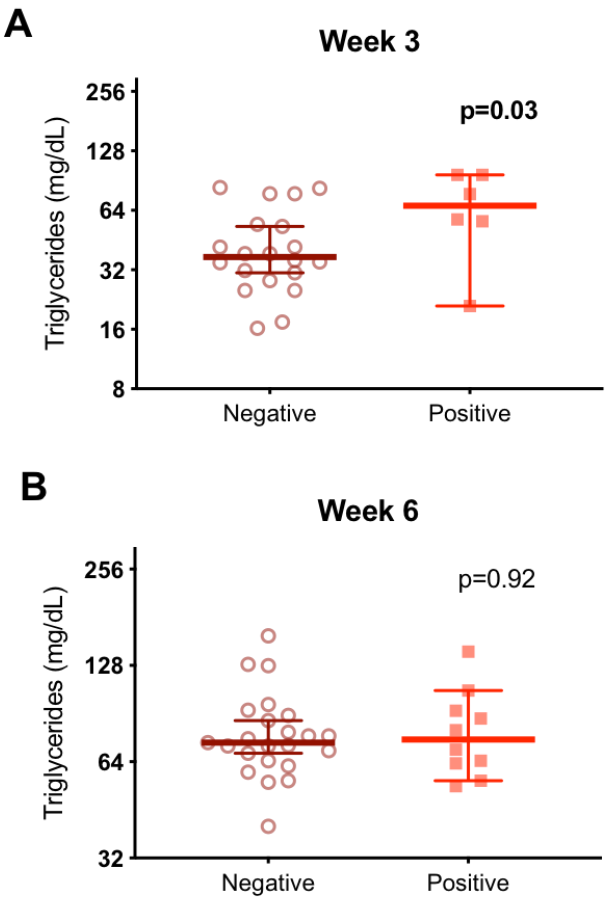

Supplemental Figure 1: In dexamethasone + fenofibrate mice, week 3 triglycerides differed by osteonecrosis status. Fasting serum triglycerides were measured at week 3 (A) and 6 (B). Graph plots serum triglycerides by osteonecrosis status in dexamethasone + fenofibrate mice. P-value was calculated using the two-tailed Mann-Whitney test. The graph show values from individual mice and the group median with 95% CI. At week 3, n= 20 (negative); n= 6 (positive). At week 6, n= 23 (negative); n= 10 (positive).

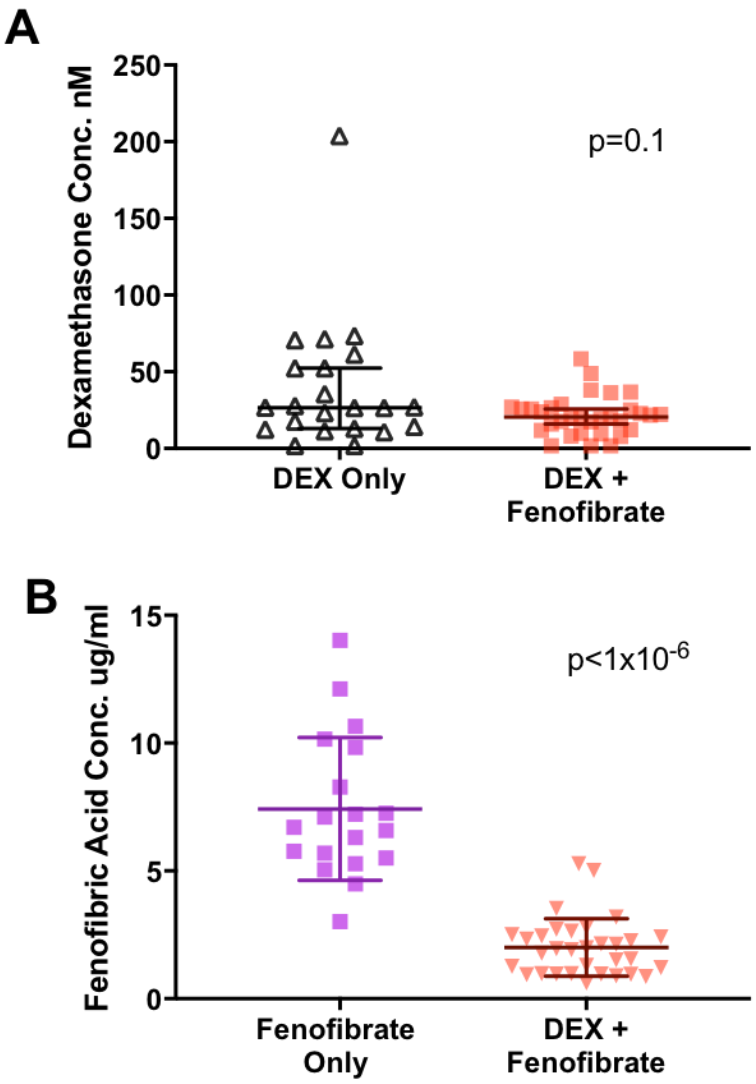

Supplemental Figure 2: Fenofibrate supplementation did not affect plasma dexamethasone. At end of treatment at week 6, dexamethasone (A) and fenofibric acid (B) were measured by HPLC-MS. P-value was calculated using the two-tailed Mann-Whitney test. The graph show values from individual mice and the group median with 95% CI. N=22 (DEX Only); n= 32 (DEX + fenofibrate).

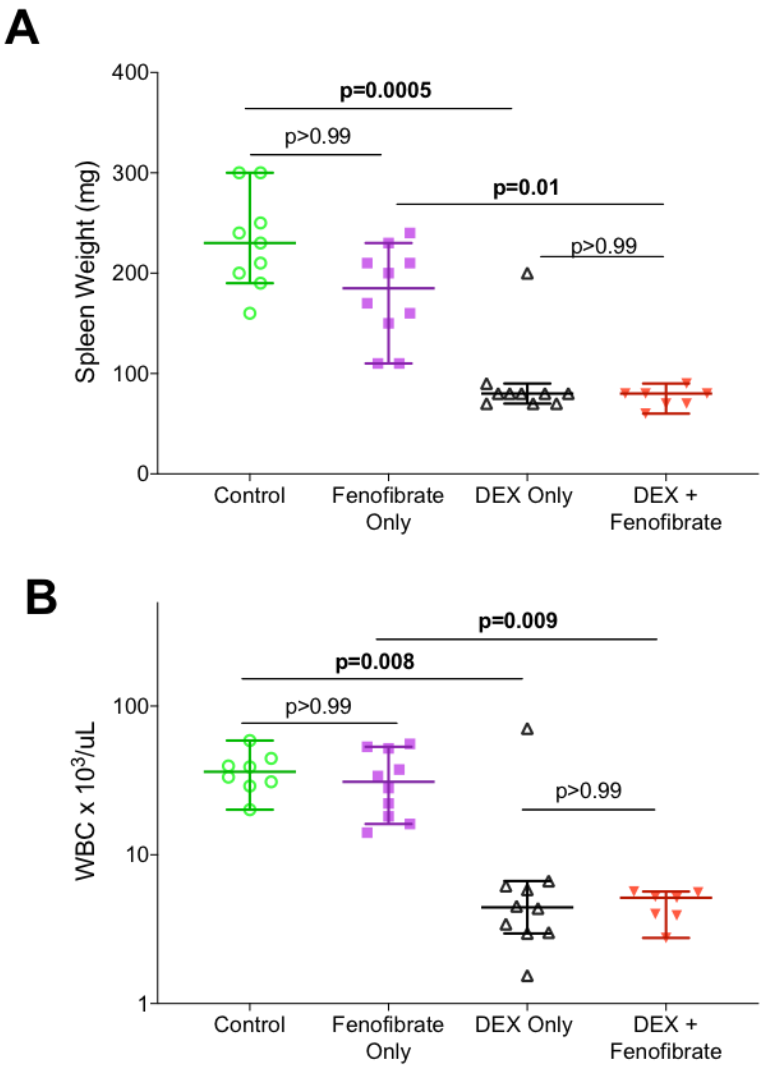

Supplemental Figure 3: Fenofibrate does not affect efficacy of dexamethasone in BCR-ABL model. At time of humane sacrifice or end experiment at day 63, spleen weight (A) and WBC count (B) were measured. N=7-10/group. Kruskal-Wallis test was used to compare groups: only p-values between relevant groups: control vs. fenofibrate-only; control vs. DEX-Only; fenofibrate-only vs. DEX+ fenofibrate; DEX-Only vs. DEX + fenofibrate. Graph show values from individual mice and the group median with 95% CI.

1. Yang L, Boyd K, Kaste SC, Kamdem Kamdem L, Rahija RJ, Relling MV. A mouse model for glucocorticoid-induced osteonecrosis: effect of a steroid holiday. Journal of orthopaedic research : official publication of the Orthopaedic Research Society. 2009 Feb;27(2):169-75.
2. Kawedia JD, Janke L, Funk AJ, Ramsey LB, Liu C, Jenkins D, et al. Substrain-specific differences in survival and osteonecrosis incidence in a mouse model. Comparative medicine. 2012 Dec;62(6):466-71.
3. Janke LJ, Liu C, Vogel P, Kawedia J, Boyd KL, Funk AJ, et al. Primary epiphyseal arteriopathy in a mouse model of steroid-induced osteonecrosis. The American journal of pathology. 2013 Jul;183(1):19-25.
4. Liu C, Janke LJ, Kawedia JD, Ramsey LB, Cai X, Mattano LA, Jr., et al. Asparaginase Potentiates Glucocorticoid-Induced Osteonecrosis in a Mouse Model. PLoS One. 2016;11(3):e0151433.
5. Finch ER, Janke LJ, Smith CA, Karol SE, Pei D, Cheng C, et al. Bloodstream infections exacerbate incidence and severity of symptomatic glucocorticoid-induced osteonecrosis. Pediatric blood & cancer. 2019 Jun;66(6):e27669.
6. Mann A, Thompson A, Robbins N, Blomkalns AL. Localization, identification, and excision of murine adipose depots. Journal of visualized experiments : JoVE. 2014 Dec 4(94).
7. Chusyd DE, Wang D, Huffman DM, Nagy TR. Relationships between Rodent White Adipose Fat Pads and Human White Adipose Fat Depots. Frontiers in nutrition. 2016;3:10.
8. Ramsey LB, Janke LJ, Payton MA, Cai X, Paugh SW, Karol SE, et al. Antileukemic Efficacy of Continuous vs Discontinuous Dexamethasone in Murine Models of Acute Lymphoblastic Leukemia. PLoS One. 2015;10(8):e0135134.
9. Williams RT, Roussel MF, Sherr CJ. Arf gene loss enhances oncogenicity and limits imatinib response in mouse models of Bcr-Abl-induced acute lymphoblastic leukemia. Proceedings of the National Academy of Sciences of the United States of America. 2006 Apr 25;103(17):6688-93.
10. Boulos N, Mulder HL, Calabrese CR, Morrison JB, Rehg JE, Relling MV, et al. Chemotherapeutic agents circumvent emergence of dasatinib-resistant BCR-ABL kinase mutations in a precise mouse model of Philadelphia chromosome-positive acute lymphoblastic leukemia. Blood. 2011 Mar 31;117(13):3585-95.
11. Ramsey LB, Janke LJ, Edick MJ, Cheng C, Williams RT, Sherr CJ, et al. Host thiopurine methyltransferase status affects mercaptopurine antileukemic effectiveness in a murine model. Pharmacogenetics and genomics. 2014 May;24(5):263-71.